In vivo immunological antitumor effect of OK-432-stimulated dendritic cell transfer after radiofrequency ablation

In vivo immunological antitumor effect of OK-432-stimulated dendritic cell transfer after radiofrequency ablation

Hidetoshi Nakagawa[1], Eishiro Mizukoshi[1], Noriho Iida[1], Takeshi Terashima[1], Masaaki Kitahara[1], Yohei Marukawa[1], Kazuya Kitamura[1], Yasunari Nakamoto[2], Kazumasa Hiroishi[3], Michio Imawari[3] and Shuichi Kaneko[1]

[1]Department of Gastroenterology, Graduate School of Medicine, Kanazawa University, Kanazawa, Ishikawa 920-8641, Japan

[2]Second Department of Internal Medicine, Faculty of Medical Sciences, University of Fukui, Fukui 910-1193, Japan

[3]Shin-yurigaoka General Hospital, Kanagawa 215-0026, Japan

Correspondence: Shuichi Kaneko, MD

Department of Gastroenterology, Graduate School of Medicine, Kanazawa University, 13-1 Takara-machi, Kanazawa, Ishikawa 920-8641, Japan

Tel: +81-76-265-2230

Fax: +81-76-234-4250

Email: skaneko@m-kanazawa.jp

ABSTRACT

Radiofrequency ablation therapy (RFA) is a radical treatment for liver cancers and induces tumor antigen-specific immune responses. In the present study, we examined the antitumor effects of focal OK-432-stimulated dendritic cell (DC) transfer combined with RFA, and analyzed the functional mechanisms involved using a murine model. C57BL/6 mice were injected subcutaneously with colon cancer cells (MC38) in their bilateral flanks. After the establishment of tumors, the subcutaneous tumor on one flank was treated using RFA and then OK-432-stimulated DCs were injected locally. The antitumor effect of the treatment was evaluated by measuring the size of the tumor on the opposite flank, and the immunological responses were assessed using tumor-infiltrating lymphocytes, splenocytes and draining lymph nodes. Tumor growth was strongly inhibited in mice that exhibited efficient DC migration after RFA and OK-432 stimulated DC transfer, as compared with mice treated with RFA alone or treatment involving immature DC transfer. We also demonstrated that the antitumor effect of this treatment depended on both CD8-positive and CD4-positive cells. On the basis of our findings, we believe that combination therapy for metastatic liver cancer consisting of OK-432-stimulated DCs in combination with RFA can proceed to clinical trials; and it is anticipated to be markedly superior to RFA single therapy.

Précis: Combination therapy involving OK-432-stimulated DC transfer and radiofrequency ablation therapy generates augmented tumor-specific immune responses

in a murine metastatic colon cancer model.

Abbreviations: RFA, radiofrequency ablation; DC, dendritic cell; HCC, hepatocellular carcinoma; TAE, transcatheter hepatic arterial embolization; TLR, Toll-like receptor; GFP, green fluorescent protein; ELISPOT, enzyme-linked immunospot; Treg, regulatory T-cell; MDSC, myeloid-derived suppressor cell; IFN-γ, interferon-γ

INTRODUCTION

Liver is one of the most common organs to which various cancers spread from their site of origin. In some types of cancer, the liver metastasis lesion is a target of surgical treatment. For instance, surgical resection of hepatic metastasis achieves longer median survival in colorectal and breast cancer patients [1,2]. However, even if the hepatic lesions are surgically treated, the prognosis of the patients is not satisfactory. As for colorectal cancers, the recurrence rate is over 50% after radical resection of metastatic lesions [3]. Moreover, at the time of initial diagnosis, only a few patients meet the criteria for hepatic resection because of unresectability, low hepatic functional reserve or poor performance status [4].

Radiofrequency ablation therapy (RFA) has been developed as a radical and minimally invasive treatment method for metastatic liver cancers. Recently, RFA has been used as an adjunct to hepatic resection, or as an alternative method to resection when surgical treatment is not feasible [5]. Additionally, it has been revealed that RFA for metastatic liver cancers generates tumor antigen-specific T-cell responses in man [6,7]. We have previously reported that RFA could also control distant tumor growth in a murine hepatocellular carcinoma (HCC) model [8].

Dendritic cells (DCs) are potent antigen-presenting cells [9]. Recently, we have established new treatments using local DC injection with transcatheter hepatic arterial embolization (TAE), and have shown that this combination therapy could induce tumor antigen-specific T-cell responses in HCC patients [10].

OK-432 is derived from the Su strain of Group A *Streptococcus pyogenes* by means of treatment with benzylpenicillin and heat [11]. OK-432 can stimulate DCs via

Toll-like receptor (TLR) 3, TLR4 and β2 integrin, and subsequently induce antigen-specific cytotoxic lymphocytes [12-14].

On the basis of these results, we hypothesized that OK-432-stimulated DC transfer is a promising candidate for an enhancer that can strongly increase the antitumor effect of RFA. We have previously demonstrated in a clinical trial that the local infusion of OK-432 by means of TAE stimulated DC levels in HCC, and could prolong recurrence-free survival [15]. However, it remains unknown as to how the transferred DCs work in combination with RFA. In the present study, we examined the antitumor effects of OK-432-stimulated DCs when combined with RFA, and analyzed the functional mechanisms involved using a murine subcutaneous colon cancer model.

MATERIALS AND METHODS

Animals

Wild-type 8–12 week old female C57BL/6J mice were obtained from Charles River Japan (Yokohama, Japan). Female C57BL/6-Tg (UBC-GFP) 30Scha/J mice were purchased from the Jackson Laboratory (Bar Harbor, ME, USA). All animal experiments were approved and performed in accordance with the Guidelines for the Care and Use of Laboratory Animals of Kanazawa University, which strictly conforms to the Guide for the Care and Use of Laboratory Animals published by the US National Institutes of Health.

Cell lines and bone marrow-derived dendritic cells

A murine colorectal cancer cell line, MC38 and hybridomas, clone GK1.5 and clone 2.43 were cultured in RPMI-1640 containing 10% fetal bovine serum (Life Technologies, Co., Carlsbad, CA, USA) supplemented with 100 μg/mL streptomycin and 100 units/ml penicillin (Wako Pure Chemical Industries Ltd., Osaka, Japan). Bone marrow-derived dendritic cells (BMDCs) were generated using 20 ng/ml of recombinant granulocyte macrophage colony-stimulating factor (R&D Systems, Minneapolis, MN, USA) as previously described [16]. OK-432 (Picibanil; Chugai Pharmaceutical Co. Ltd., Tokyo, Japan) was loaded into the supernatant from days 6–7 of the BMDC generation period at a concentration of 5 μg/ml.

In vitro evaluation of phagocytic activity by dendritic cells

MC38 cells were labeled with DiD dye (Life Technologies) according to the

manufacturer's instructions followed by heat treatment at 80°C for 90 seconds. OK-432-stimulated or immature DCs were co-incubated with the treated MC38 cells for 3 hours at a ratio of 1:1. After incubation, the cell suspensions were observed using a fluorescence microscope (BZ9000: Keyence, Osaka, Japan) and analyzed by means of FACSCalibur (BD Immuno-Cytometry System, San Jose, CA, USA).

Animal model

Bilateral flanks of C57BL/6 mice were each injected subcutaneously with 1×10^6 MC38 cells. Seven days after injection, after they had grown to 5–6 mm in diameter, the subcutaneous tumors on one flank were treated using RFA, and 1×10^7 immature DCs or 1×10^7 OK-432-stimulated DCs were injected into the treated tumors at 24 hours after RFA. After this, the volume of the untreated tumor on the contralateral flank was evaluated over a period of 10 days. Tumor volumes were calculated using the following formula: tumor volume (mm^3) = (longest diameter) × (shortest diameter)^2 / 2.

Radiofrequency ablation

Mice bearing tumors were anesthetized with an intraperitoneal injection of pentobarbital (Kyoritsu Seiyaku, Tokyo, Japan), and the skin on the tumor was cut. Subsequently, an expandable RFA needle was inserted into the tumor, which was treated using a radiofrequency generator (RITA 500PA; RITA Medical Systems, Inc., Fremont, CA, USA). During the use of this system, the intratumor temperature was maintained at 70–90°C, and the current was turned off when the tumor exhibited heat denaturation.

Flow cytometry

The DCs were detected by means of staining with anti-CD11c antibodies (Life technologies). The lymphocytes in the draining lymph node were stained with anti-CD4 antibodies, anti-CD8 antibodies, anti-CD11c antibodies and anti-CD69 antibodies (BD Bioscience, San Diego, CA, USA). The splenocytes were stained with anti-CD4 antibodies, anti-CD8 antibodies, CD11c antibodies, anti-NK1.1 antibodies, CD45 antibodies (BD Bioscience), anti-Gr-1 antibodies, and anti-CD11b antibodies and mouse regulatory T-cell staining solution (BioLegend, San Diego, CA, USA). The stained samples were analyzed using FACSAria II (BD Immuno-Cytometry System).

Immunohistochemical assay

The draining lymph nodes and the observed tumors were embedded in Sakura Tissue-Tek optimum cutting temperature compound (Sakura Finetek Japan Co., Ltd., Tokyo, Japan) for frozen sectioning. Tissue sections were fixed at −20°C in methanol for 10 minutes. The draining lymph nodes were stained using rabbit anti-GFP antibody (Abcam, Cambridge, UK) that were detected using an EnVision+/HRP kit (Dako, Glostrup, Denmark). The observed tumors were stained with anti-CD4 and anti-CD8a (BD Bioscience), which were detected using the Nichirei Histofine Simple Stain Mouse Max PO (Rat) system (Nichirei Co., Tokyo, Japan) or the Vectastain ABC kit (Vector Laboratory, Inc., Burlingame, CA, USA).

Interferon gamma enzyme-linked immunospot assay

The splenocytes, the tumor-infiltrating lymphocytes (TILs) in the untreated tumors that were isolated by mechanical homogenizations and density gradient centrifugations, and the lymphocytes in the draining lymph nodes were loaded into the interferon gamma

enzyme-linked immunospot assay to estimate the tumor-specific immune reactions, as previously described [8,17]. Briefly, 3×10^5 lymphocytes or 1×10^5 TILs were incubated for 24 hours with or without 6×10^5 MC38 lysates, which were prepared through five cycles of rapid freezing in liquid nitrogen, thawing at 55°C and centrifugation. The number of MC38-specific IFN-γ spots was determined by subtracting the number of spots incubated without MC38 lysates from the number of spots incubated with MC38 lysates. For CD4 or CD8 depletion, we used magnetic CD4-beads or CD8-beads (Miltenyi Biotec, Bergisch Gladbach, Germany).

In vivo CD4/CD8 depletion

For in vivo CD4 or CD8 depletion, B6 mice were injected intraperitoneally with 200 μg of purified monoclonal antibodies specific for CD4 or CD8 at 1 day before and 3 days after RFA treatment; the monoclonal antibodies were prepared from GK1.5 hybridoma and 2.43 hybridoma, respectively [18]. The depletion was confirmed by flow cytometry using peripheral blood lymphocytes stained with anti-CD4 and anti-CD8 antibodies.

Statistical analysis

The data obtained were analyzed statistically using the t test or one-way analysis of variance followed by Tukey's multiple comparison test. A P value < 0.05 was considered as being statistically significant.

RESULTS

Migration efficacy and phagocytic ability of OK-432-stimulated DCs

We employed OK-432 as a modifying agent for DCs, because we have previously shown in clinical studies that OK-432 prolonged recurrence-free survival after combination therapy involving DC injection with TAE for HCC patients [10,15]. We first confirmed that the OK-432-stimulated murine DCs showed higher expression of maturation markers such as CD40, CD80, CD86, MHC class II and CCR7 (Supplementary Fig. 1), as previously reported [19,20].

To evaluate their phagocytic abilities, we incubated the immature DCs and the OK-432-stimulated DCs with MC38 tumor cells. Heat-treated MC38 cells were taken up well by both immature DCs and OK-432-stimulated DCs, as compared with non-treated MC38 cells (Fig. 1a-c). In addition, the phagocytic ability of OK-432-stimulated DCs was not inferior to that of immature DCs. These results were consistent with the dextran uptake assay (Supplementary Fig. 2) and our previous data on human monocyte-derived DCs [15]. Since heat-treated MC38 cells were thought to be in a similar condition to those in the MC38 tumor in mice treated with RFA, OK-432-stimulated DCs were expected to effectively phagocytose RFA-treated MC38 tumor cells in vivo.

We next estimated the kinetics of the transferred DCs in mice bearing subcutaneous MC38 tumors treated with RFA. Immature DCs or OK-432-stimulated DCs that were derived from GFP-Tg mice were injected intratumorally at 24 hours after RFA treatment, and the subcutaneous tumors and the lymph nodes were harvested at 3 days after RFA. According to the immunohistochemical study involving the detection of GFP, the

inguinal lymph node on the RFA-treated flank was thought to be the draining lymph node (Supplementary Fig. 3). Additionally, the number of transferred DCs in the draining lymph nodes was significantly higher in the mice treated with the OK-432-stimulated DCs than in those treated with the immature DCs (Fig. 1d, e). Our experimental results attested to the fact that the OK-432-stimulated DCs had both sufficient phagocytic ability and higher migration efficacy.

Effect of RFA in combination with the injection of OK-432-stimulated DCs on tumor growth

OK-432-stimulated DCs were used in combination therapy with RFA in this murine model (Fig. 2a). Namely, BMDCs stimulated with OK-432 were injected into RFA treated tumor at 24 hours after RFA treatment. We compared four groups of tumor bearing mice as follows: 1) no treatment; 2) RFA only; 3) RFA with the injection of immature DCs; and 4) RFA with the injection of OK-432-stimulated DCs. Tumor volumes were measured for 10 days after treatment/no treatment. On the day after RFA, the treated tumors were covered with scars, started to shrink, and had disappeared macroscopically at 4 days after RFA in all of the groups. This indicated that RFA treatment was highly effective for focal lesions. The injected DCs were detected in the treated tumors (Supplementary Fig. 3). With regard to the untreated tumors, as we previously reported, the group treated with RFA only showed an antitumor effect against distant tumors. The injection of immature DCs combined with RFA did not show any additional enhancement of the antitumor effect. On the other hand, the volumes of the untreated tumors in the group that underwent RFA combined with the injection of OK-432-stimulated DCs were strongly suppressed (P<0.001) relative to other groups

(Fig. 2b).

Recruitment of antigen-specific lymphocyte fractions in both splenocytes and tumor by injected OK-432-stimulated DCs

Ten days after RFA, the tumors and the spleens were harvested and analyzed using immunohistochemical staining. We examined the number of tumor-infiltrating CD4-positive or CD8-positive cells in the tumors by means of immunohistochemistry. The infiltration of these cells into the untreated tumors was found to be promoted by RFA. The injection of OK-432-stimulated DCs after RFA induced the additional recruitment of CD8-positive cells into the untreated tumors (Fig. 3a, b). CD11c-, CD11b- and NK1.1-positive cells were very marginal and showed no differences in number among the four groups (data not shown).

Systemically, in terms of analyzing splenocytes with flow cytometry, the numbers of CD4-positive and CD8-positive cells increased in the group treated with RFA in combination with OK-432-stimulated DCs. On the other hand, the CD11c and NK1.1 fractions, which were considered as DCs and NK cells, respectively, presented no difference among the four groups (Fig. 3c). In addition, we examined the effect of the injection of OK-432-stimulated DCs after RFA on inhibitory blood cells such as regulatory T-cells (Tregs) and myeloid-derived suppressor cells (MDSCs) (Fig. 3c). Among CD4-positive cells, significantly fewer Tregs were detected in the group treated with RFA in combination with OK-432-stimulated DCs than in the group treated with RFA in combination with immature DCs. In the analysis of MDSCs, their rates of occurrence were not affected by treatment with either RFA alone or RFA in combination with DCs. Taking these results together, we concluded that treatment with RFA

combined with OK-432-stimulated DCs enhanced the number of CD4- or CD8-positive T cells and reduced the Treg/CD4 ratio, but did not influence MDSC numbers.

Furthermore, we examined the number of tumor-specific IFN-γ-producing cells at 10 days after RFA using the ELISPOT assay. The number of IFN-γ-producing cells among splenocytes and TILs showed the same trend as the level of tumor growth control among the four groups (Fig. 3d); the group treated with RFA in combination with injected OK-432 DCs showed the most abundant specific spots. These results suggested that the augmented antitumor effects of RFA combined with OK-432-stimulated DCs depended in large part on tumor-specific immune responses by CD4 cells or CD8 cells.

Evaluation of tumor-specific immune responses in the draining lymph node after OK-432-stimulated DC transfer

CD4 T- and CD8 T-cells are now thought to have an important antitumor effect as a result of the OK-432-stimulated DC transfer. To elucidate the priming of the antigen-specific immune response, we analyzed the draining lymph nodes at 3 days after RFA focusing on CD4-positive or CD8-positive cells. CD69, the early activation marker, on CD4-positive and CD8-positive cells were examined and compared between the immature DC transfer group and the OK-432-stimulated DC transfer group. It was found that CD69 expression on both CD4-positive and CD8-positive cells were elevated in the OK-432-stimulated DC transfer group (Fig. 4a, b). The activations were also demonstrated to be tumor-specific using the IFN-γ ELISPOT assay in which each CD4-negative and CD8-negative fraction was applied to the assay and both showed tumor-specific IFN-γ secretions (Fig. 4c).

Evaluation of the relationship between CD4-positive and CD8-positive cells and the antitumor effects of RFA and OK-432-stimulated DC transfer

We have demonstrated that combination therapy involving RFA and OK-432-stimulated DC transfer might generate enhanced antitumor effects via tumor-specific CD4-positive and CD8-positive cells. To obtain further evidence, we carried out in vivo CD4 or CD8 depletion studies in mice. Initially, we confirmed CD4 or CD8 depletion in the control in vivo study (Supplementary Fig. 4). The CD4-positive and CD8-positive fractions in the peripheral blood were greatly depleted at 7 days after injection of the antibodies. The experimental schedule was determined as follows. The depletion antibodies were injected at 1 day before and 3 days after RFA, and the tumors that were not treated with RFA were observed for 10 days. In addition, the draining lymph nodes were harvested at 3 days after RFA and analyzed (Supplementary Fig. 5). The antitumor effects of RFA treatment and the augmented effects from OK-432-stimulated DCs were cancelled out by depletion of both CD4 and CD8 cells (Fig. 5a). In the CD4 depletion study, there was no priming of the antitumor effect in the draining lymph nodes (Fig. 5b; Supplementary Fig. 6). On the other hand, in the CD8 depletion study CD4 cells were activated with tumor-specificities in the draining lymph node in both groups, and the activation was stronger in the OK-432 stimulated DC transfer group (Fig. 5b; Supplementary Fig. 6). Tumor-specific reactions were also demonstrated in the splenocytes and the TILs at 10 days after RFA. There was a tendency for OK-432 DC transfer treatment to result in the recruitment of increased numbers of tumor-specific lymphocytes into the tumor on the opposite flank (P=0.184; Fig. 5c). These results indicated that the tumor-specific activation of CD8 cells was necessary for the antitumor effect, and was completely dependent on help from the CD4 cells.

DISCUSSION

In the past decade, cytotoxic agents and molecular-targeted therapies have been developed, and the treatment outcomes for various cancers have improved. However, few patients with advanced cancers have been completely cured and thus new strategies for anticancer therapy are required. Immunotherapy is considered to have the potential to effectively treat such advanced cancers, and many different approaches have been explored. For the utilization of the adoptive immune response in a cancer therapy, DCs are a key constituent of the immune system. This is because of their natural potential to present tumor-associated antigens to CD4^{+} and CD8^{+} lymphocytes, and also to control both immune tolerance and immunity [21]. Thus, DCs are considered as an important target for cancer immunotherapy. Many trials and studies have been carried out regarding immunotherapy for cancer using DCs, some of which have been reported to have pronounced effects [22-25]. In recent studies, it has been revealed that RFA treatment induces tumor-specific T-cell responses, which is known as the abscopal effect; this has been mainly reported in radiotherapy studies and is augmented with combined immunotherapies [26,27]. Brok et al. have previously reported on the vaccination effects of combination therapy involving RFA and CTLA-4 antibody [28].

To our knowledge, this is the first study that has demonstrated using a murine metastatic cancer model that RFA in combination with focal DC injection could enhance the antitumor effects of RFA alone. Our results showed that immature DCs made no additional immunological contribution to RFA. In the analysis of draining lymph nodes, few transferred DCs were detected after the injection of immature DCs. It appeared that immature DCs did not act as sentinels in the adoptive immune system, partially because

they exhibited low expression of CCR7 (the main molecule that promotes DC migration [29]), even though elevation of CCR7 expression using OK-432 was very modest in our study. There is another possibility, namely that immature DCs are easily lysed and excluded by the host immune system [30]. On the other hand, mature DCs can escape cell lysis [31].

Utilization of OK-432-stimulated DCs improved the number of migrating transferred DCs in the present study. These DCs, which could act as sentinels for immunity, induced expansion in the number of tumor-specific lymphocytes in the draining lymph nodes, in the splenocytes and in the distant non-treated tumors, without systemic expansion of inhibitory cells such as Tregs or MDSCs. We also demonstrated that these augmented antitumor effects after OK-432-stimulated DC transfer were primed in the draining lymph nodes with tumor-specific activations of CD4-positive cells and CD8-positive cells; it was proved that without CD4-positive cells or CD8-positive cells, both the antitumor effect by RFA and the additional effect of the injection of OK-432-stimulated DCs disappeared completely. In addition, the in vivo CD4 depletion study revealed that tumor-specific activations of CD8-positive cells were not seen in the draining lymph nodes in both groups after the injection of immature DCs and OK-432-stimulated DC injection; in other words, tumor-specific CD8 activation depended on CD4-positive cells entirely. In the CD8 depletion study, on the other hand, we found that tumor-specific CD4-positive cells appeared in the draining lymph nodes, the splenocyte population and the untreated tumor on the opposite flank, and these lymphocytes were considered to be CD4 positive cells. In the tumor-infiltrating lymphocytes, there was a tendency for more tumor-specific CD4-positive cells to be recruited after treatment involving OK-432-stimulated DC transfer. Many researchers

have demonstrated the contribution of CD4 cells to cytotoxicity [32,33]. However, in our experimental models, tumor-specific CD4 positive cells were not observed to contribute to the antitumor effect. Summarizing the above, in our study, the CD4-positive cells were required for the priming of the immune responses, and the CD8-positive cells acted as the effector cells after help from the CD4-positive cells.

In conclusion we consider, on the basis of our preclinical findings regarding combination therapy involving OK-432-stimulated DCs with RFA for the treatment of metastatic liver cancer that clinical trials can now proceed. It is anticipated that this combination therapy will be markedly superior to RFA single therapy.

ACKNOWLEDGMENTS

CONFLICT OF INTEREST STATEMENT

REFERENCES

1. Ruiterkamp J, Ernst MF, de Munck L, van der Heiden-van der Loo M, Bastiaannet E, van de Poll-Franse LV, Bosscha K, Tjan-Heijnen VC, Voogd AC (2011) Improved survival of patients with primary distant metastatic breast cancer in the period of 1995-2008. A nationwide population-based study in the Netherlands. Breast Cancer Res Treat 128 (2):495-503. doi:10.1007/s10549-011-1349-x

2. Simmonds PC, Primrose JN, Colquitt JL, Garden OJ, Poston GJ, Rees M (2006) Surgical resection of hepatic metastases from colorectal cancer: a systematic review of published studies. Br J Cancer 94 (7):982-999. doi:10.1038/sj.bjc.6603033

3. Nordlinger B, Guiguet M, Vaillant JC, Balladur P, Boudjema K, Bachellier P, Jaeck D (1996) Surgical resection of colorectal carcinoma metastases to the liver. A prognostic scoring system to improve case selection, based on 1568 patients. Association Francaise de Chirurgie. Cancer 77 (7):1254-1262

4. Bentrem DJ, Dematteo RP, Blumgart LH (2005) Surgical therapy for metastatic disease to the liver. Annu Rev Med 56:139-156. doi:10.1146/annurev.med.56.082103.104630

5. Meyers MO, Sasson AR, Sigurdson ER (2003) Locoregional strategies for colorectal hepatic metastases. Clin Colorectal Cancer 3 (1):34-44. doi:10.3816/CCC.2003.n.010

6. Napoletano C, Taurino F, Biffoni M, De Majo A, Coscarella G, Bellati F, Rahimi H, Pauselli S, Pellicciotta I, Burchell JM, Gaspari LA, Ercoli L, Rossi P, Rughetti A (2008) RFA strongly modulates the immune system and anti-tumor immune responses in metastatic liver patients. Int J Oncol 32 (2):481-490

7. Nobuoka D, Motomura Y, Shirakawa H, Yoshikawa T, Kuronuma T, Takahashi M,

Nakachi K, Ishii H, Furuse J, Gotohda N, Takahashi S, Nakagohri T, Konishi M, Kinoshita T, Komori H, Baba H, Fujiwara T, Nakatsura T (2012) Radiofrequency ablation for hepatocellular carcinoma induces glypican-3 peptide-specific cytotoxic T lymphocytes. Int J Oncol 40 (1):63-70. doi:10.3892/ijo.2011.1202

8. Iida N, Nakamoto Y, Baba T, Nakagawa H, Mizukoshi E, Naito M, Mukaida N, Kaneko S (2010) Antitumor effect after radiofrequency ablation of murine hepatoma is augmented by an active variant of CC Chemokine ligand 3/macrophage inflammatory protein-1alpha. Cancer Res 70 (16):6556-6565. doi:10.1158/0008-5472.CAN-10-0096

9. Banchereau J, Briere F, Caux C, Davoust J, Lebecque S, Liu YJ, Pulendran B, Palucka K (2000) Immunobiology of dendritic cells. Annu Rev Immunol 18:767-811. doi:10.1146/annurev.immunol.18.1.767

10. Nakamoto Y, Mizukoshi E, Tsuji H, Sakai Y, Kitahara M, Arai K, Yamashita T, Yokoyama K, Mukaida N, Matsushima K, Matsui O, Kaneko S (2007) Combined therapy of transcatheter hepatic arterial embolization with intratumoral dendritic cell infusion for hepatocellular carcinoma: clinical safety. Clin Exp Immunol 147 (2):296-305. doi:10.1111/j.1365-2249.2006.03290.x

11. Ryoma Y, Moriya Y, Okamoto M, Kanaya I, Saito M, Sato M (2004) Biological effect of OK-432 (picibanil) and possible application to dendritic cell therapy. Anticancer Res 24 (5C):3295-3301

12. Nakahara S, Tsunoda T, Baba T, Asabe S, Tahara H (2003) Dendritic cells stimulated with a bacterial product, OK-432, efficiently induce cytotoxic T lymphocytes specific to tumor rejection peptide. Cancer Res 63 (14):4112-4118

13. Okamoto M, Oshikawa T, Tano T, Ahmed SU, Kan S, Sasai A, Akashi S, Miyake K, Moriya Y, Ryoma Y, Saito M, Sato M (2006) Mechanism of anticancer host response

induced by OK-432, a streptococcal preparation, mediated by phagocytosis and Toll-like receptor 4 signaling. J Immunother 29 (1):78-86

14. Hovden AO, Karlsen M, Jonsson R, Appel S (2012) The bacterial preparation OK432 induces IL-12p70 secretion in human dendritic cells in a TLR3 dependent manner. PLoS One 7 (2):e31217. doi:10.1371/journal.pone.0031217

15. Nakamoto Y, Mizukoshi E, Kitahara M, Arihara F, Sakai Y, Kakinoki K, Fujita Y, Marukawa Y, Arai K, Yamashita T, Mukaida N, Matsushima K, Matsui O, Kaneko S (2011) Prolonged recurrence-free survival following OK432-stimulated dendritic cell transfer into hepatocellular carcinoma during transarterial embolization. Clin Exp Immunol 163 (2):165-177. doi:10.1111/j.1365-2249.2010.04246.x

16. Inaba K, Inaba M, Romani N, Aya H, Deguchi M, Ikehara S, Muramatsu S, Steinman RM (1992) Generation of large numbers of dendritic cells from mouse bone marrow cultures supplemented with granulocyte/macrophage colony-stimulating factor. J Exp Med 176 (6):1693-1702

17. Mizukoshi E, Nakamoto Y, Marukawa Y, Arai K, Yamashita T, Tsuji H, Kuzushima K, Takiguchi M, Kaneko S (2006) Cytotoxic T cell responses to human telomerase reverse transcriptase in patients with hepatocellular carcinoma. Hepatology 43 (6):1284-1294. doi:10.1002/hep.21203

18. Nakamoto Y, Suda T, Momoi T, Kaneko S (2004) Different procarcinogenic potentials of lymphocyte subsets in a transgenic mouse model of chronic hepatitis B. Cancer Res 64 (9):3326-3333

19. Okamoto M, Furuichi S, Nishioka Y, Oshikawa T, Tano T, Ahmed SU, Takeda K, Akira S, Ryoma Y, Moriya Y, Saito M, Sone S, Sato M (2004) Expression of toll-like receptor 4 on dendritic cells is significant for anticancer effect of dendritic cell-based

immunotherapy in combination with an active component of OK-432, a streptococcal preparation. Cancer Res 64 (15):5461-5470. doi:10.1158/0008-5472.CAN-03-4005

20. Hill KS, Errington F, Steele LP, Merrick A, Morgan R, Selby PJ, Georgopoulos NT, O'Donnell DM, Melcher AA (2008) OK432-activated human dendritic cells kill tumor cells via CD40/CD40 ligand interactions. J Immunol 181 (5):3108-3115

21. Banchereau J, Steinman RM (1998) Dendritic cells and the control of immunity. Nature 392 (6673):245-252. doi:10.1038/32588

22. Timmerman JM, Czerwinski DK, Davis TA, Hsu FJ, Benike C, Hao ZM, Taidi B, Rajapaksa R, Caspar CB, Okada CY, van Beckhoven A, Liles TM, Engleman EG, Levy R (2002) Idiotype-pulsed dendritic cell vaccination for B-cell lymphoma: clinical and immune responses in 35 patients. Blood 99 (5):1517-1526

23. Banchereau J, Palucka AK, Dhodapkar M, Burkeholder S, Taquet N, Rolland A, Taquet S, Coquery S, Wittkowski KM, Bhardwaj N, Pineiro L, Steinman R, Fay J (2001) Immune and clinical responses in patients with metastatic melanoma to CD34(+) progenitor-derived dendritic cell vaccine. Cancer Res 61 (17):6451-6458

24. Okada H, Kalinski P, Ueda R, Hoji A, Kohanbash G, Donegan TE, Mintz AH, Engh JA, Bartlett DL, Brown CK, Zeh H, Holtzman MP, Reinhart TA, Whiteside TL, Butterfield LH, Hamilton RL, Potter DM, Pollack IF, Salazar AM, Lieberman FS (2011) Induction of CD8+ T-cell responses against novel glioma-associated antigen peptides and clinical activity by vaccinations with {alpha}-type 1 polarized dendritic cells and polyinosinic-polycytidylic acid stabilized by lysine and carboxymethylcellulose in patients with recurrent malignant glioma. J Clin Oncol 29 (3):330-336. doi:10.1200/JCO.2010.30.7744

25. Suso EM, Dueland S, Rasmussen AM, Vetrhus T, Aamdal S, Kvalheim G,

Gaudernack G (2011) hTERT mRNA dendritic cell vaccination: complete response in a pancreatic cancer patient associated with response against several hTERT epitopes. Cancer Immunol Immunother 60 (6):809-818. doi:10.1007/s00262-011-0991-9

26. Frey B, Weiss EM, Rubner Y, Wunderlich R, Ott OJ, Sauer R, Fietkau R, Gaipl US (2012) Old and new facts about hyperthermia-induced modulations of the immune system. Int J Hyperthermia 28 (6):528-542. doi:10.3109/02656736.2012.677933

27. Rubner Y, Wunderlich R, Ruhle PF, Kulzer L, Werthmoller N, Frey B, Weiss EM, Keilholz L, Fietkau R, Gaipl US (2012) How does ionizing irradiation contribute to the induction of anti-tumor immunity? Front Oncol 2:75. doi:10.3389/fonc.2012.00075

28. den Brok MH, Sutmuller RP, van der Voort R, Bennink EJ, Figdor CG, Ruers TJ, Adema GJ (2004) In situ tumor ablation creates an antigen source for the generation of antitumor immunity. Cancer Res 64 (11):4024-4029. doi:10.1158/0008-5472.CAN-03-3949

29. Forster R, Schubel A, Breitfeld D, Kremmer E, Renner-Muller I, Wolf E, Lipp M (1999) CCR7 coordinates the primary immune response by establishing functional microenvironments in secondary lymphoid organs. Cell 99 (1):23-33

30. Ferlazzo G, Tsang ML, Moretta L, Melioli G, Steinman RM, Munz C (2002) Human dendritic cells activate resting natural killer (NK) cells and are recognized via the NKp30 receptor by activated NK cells. J Exp Med 195 (3):343-351

31. Morandi B, Mortara L, Chiossone L, Accolla RS, Mingari MC, Moretta L, Moretta A, Ferlazzo G (2012) Dendritic cell editing by activated natural killer cells results in a more protective cancer-specific immune response. PLoS One 7 (6):e39170. doi:10.1371/journal.pone.0039170

32. Ab BK, Kiessling R, Van Embden JD, Thole JE, Kumararatne DS, Pisa P, Wondimu

A, Ottenhoff TH (1990) Induction of antigen-specific CD4+ HLA-DR-restricted cytotoxic T lymphocytes as well as nonspecific nonrestricted killer cells by the recombinant mycobacterial 65-kDa heat-shock protein. Eur J Immunol 20 (2):369-377. doi:10.1002/eji.1830200221

33. Bourgault I, Gomez A, Gomard E, Picard F, Levy JP (1989) A virus-specific CD4+ cell-mediated cytolytic activity revealed by CD8+ cell elimination regularly develops in uncloned human antiviral cell lines. J Immunol 142 (1):252-256

FIGURE LEGENDS

Figure 1: Effects of OK-432 on murine bone marrow-derived DCs. (a) OK-432-stimulated DCs or immature DCs were co-incubated for 3 hours with MC38 cells untreated or treated at 80°C for 90 seconds after staining with DiD dye. After incubation, DC and MC38 cells were observed using a fluorescence microscope. Arrowheads indicate MC38 derivatives being phagocytosed by DCs. No tx, untreated MC38 cells; Heat tx, heat-treated MC38 cells; Bar, 20μm. (b) and (c) Co-incubated MC38 cells and DCs were stained with anti-CD11c antibodies and analyzed using flow cytometry. The histograms show the DiD fluorescent intensity of the CD11c positive fractions. The percentages of DiD+CD11c+ cells in the CD11c+ cell population are also shown in a column graph. The experiments were performed five times and representative results are shown. Data are presented as the mean ± SE. *, P<0.05. (d) The migration abilities of the DCs after intratumoral transfer were evaluated. The draining lymph nodes were harvested at 3 days after RFA followed by the DC transfer. Frozen sections were prepared and stained with anti-GFP antibodies. Arrows indicate the GFP-positive cells in the lymph nodes. Bar, 20μm. (e) The draining lymph nodes were also analyzed using flow cytometry after staining with anti-CD11c antibodies. Data were obtained from six mice in each group. Percentages of GFP+CD11c+ cell are presented as the mean ± SE. **, P<0.01.

Figure 2: Impact of injection of OK-432-stimulated DCs into murine MC38 subcutaneous tumors. (a) RFA was administered to a tumor on one flank followed by injection of 1×10^{7} DCs into the treated tumor. The untreated tumor on the opposite flank

was observed for 10 days. The solid arrowheads indicate the treatment intervention sites and the open arrowhead indicates the observed untreated tumor. (b) The tumor volumes were compared among the four groups as follows: 1) no treatment; 2) RFA only; 3) RFA in combination with immature DC injection; and 4) RFA in combination with OK-432-stimulated DC injection. n=8 mice per group. The data are presented as the mean ± SE. *, P<0.05; **, P<0.001.
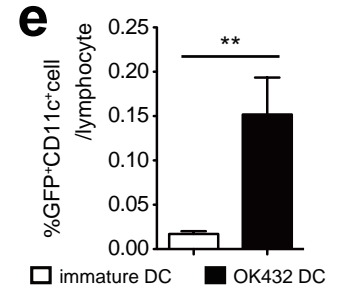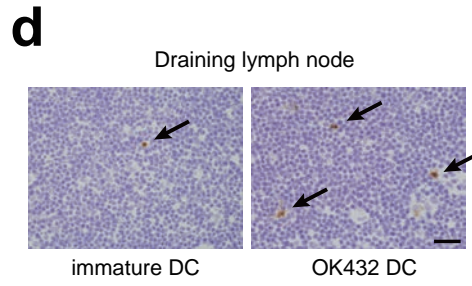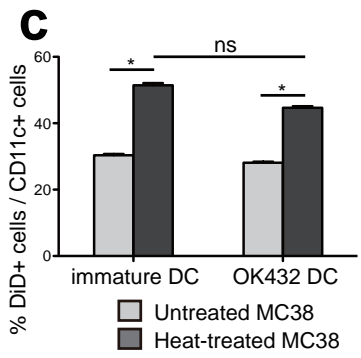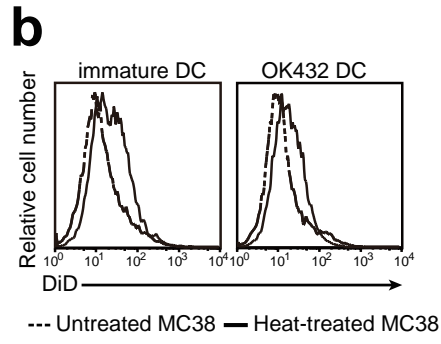
Figure 3: Analysis of the tumor-infiltrating lymphocytes and the splenocytes after combination therapy with RFA and DC injection. (a) CD4-positive and CD8-positive cells in the observed untreated tumors were detected using immunohistochemistry at 10 days after RFA. The black bar represents 50 μm. (b) The number of positive cells was counted using a microscope. This was achieved by counting the number of cells in six randomly chosen tumor areas at 400-fold magnification. Three mice were used in each group. The data are presented as the mean ± SE. ***, P<0.001; ns, not significant. (c) Ten days after RFA, splenocytes were stained with anti-CD4, anti-CD8, anti-NK1.1 and anti-CD11c antibodies and analyzed using flow cytometry. Regulatory T cells (Tregs) defined as $CD4^+CD25^+Foxp3^+$ cells and myeloid-derived suppressor cells (MDSCs) defined as $CD11b^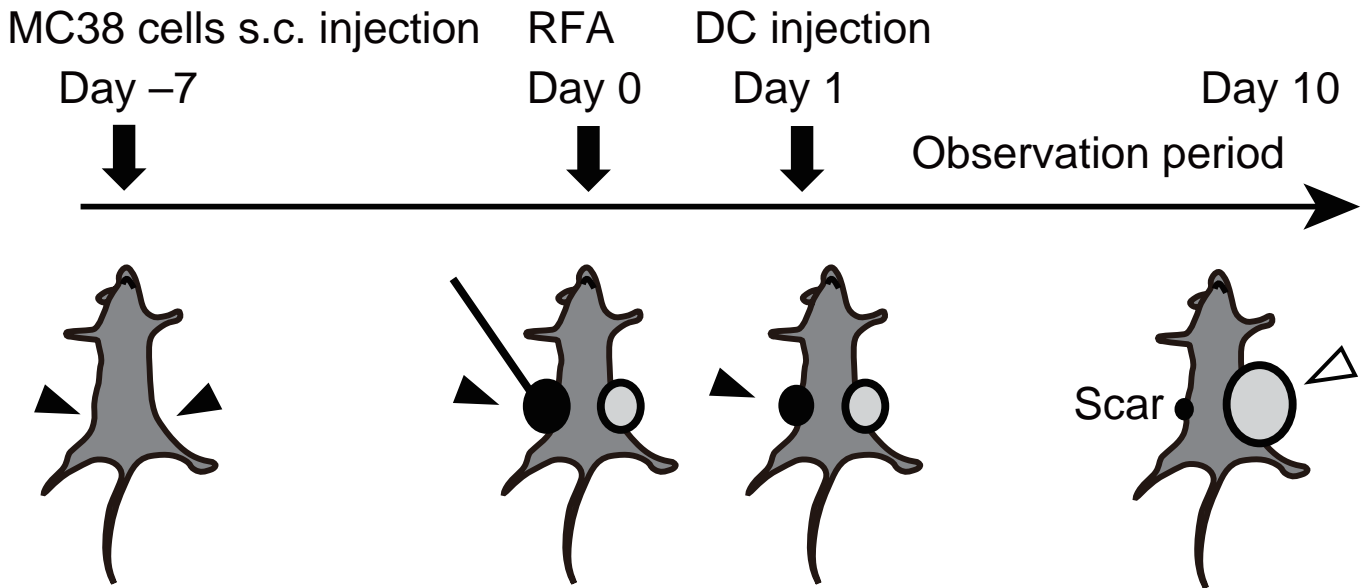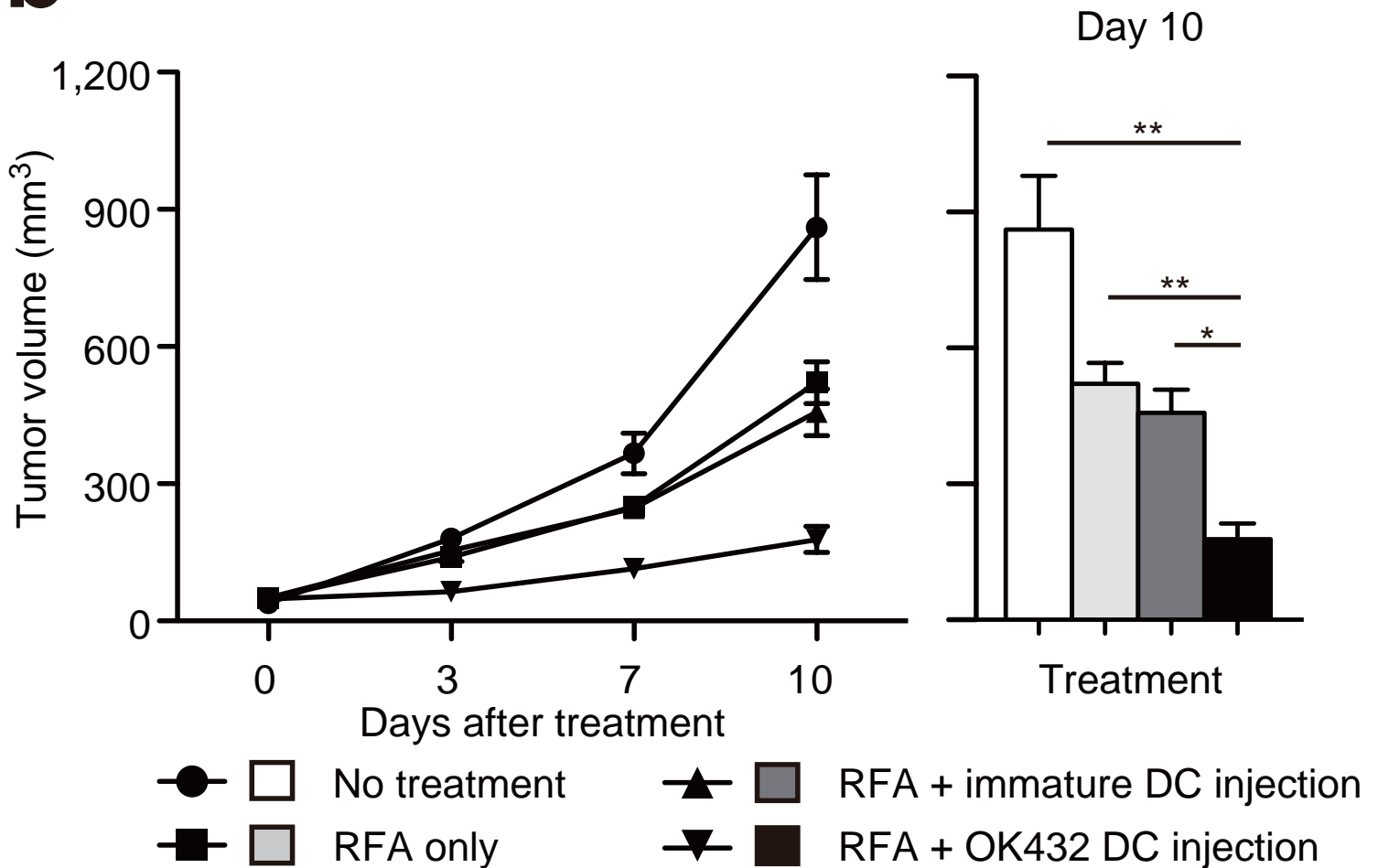+Gr-1^+$ cells were counted and compared among the four groups. Six mice were analyzed in each group. The data are presented as the mean ± SE. *, P<0.05; **, P<0.01; ***, P<0.001; ns, not significant. (d) Immune responses by the splenocytes and the tumor-infiltrating lymphocytes (TILs) were examined by means of the IFN-γ enzyme-linked immunospot (ELISPOT) assay using MC38 lysate. In the assay for TILs, 1×10^5 TILs were mixed with 2×10^5 splenocytes from B6 mice and applied to the well.

Six mice were analyzed in each group. The data are presented as the mean ± SE. **, P<0.01; ***, P<0.001; ns, not significant.
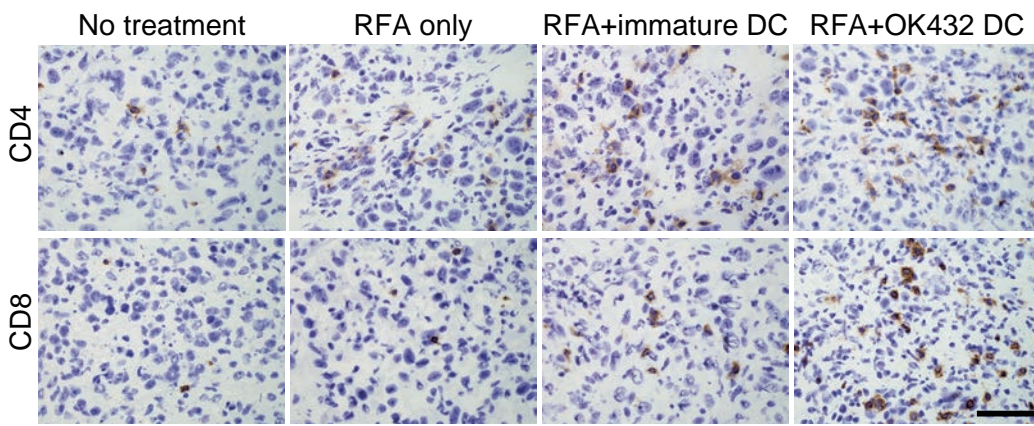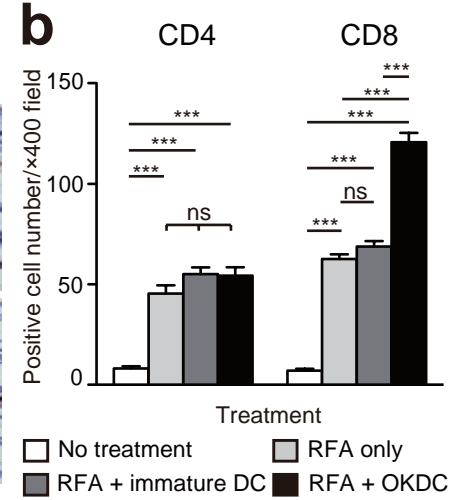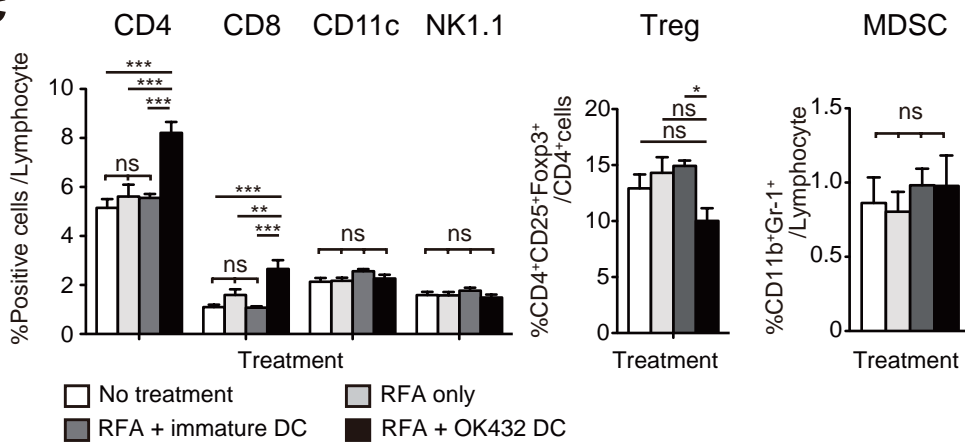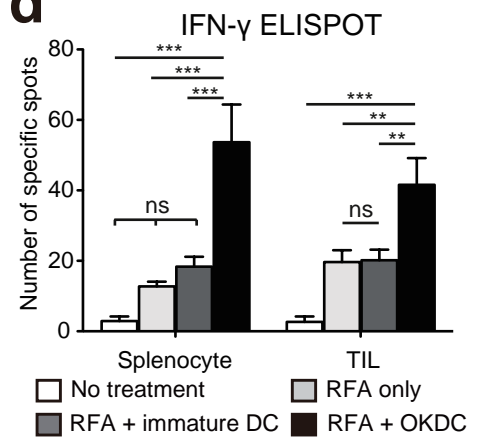
Figure 4: Antigen-specific activation of both CD4-positive and CD8-positive cells in the draining lymph node. (a) Three days after RFA followed by DC transfer the draining lymph node was harvested and analyzed by staining with anti-CD4 antibodies, anti-CD8 antibodies and anti-CD69 antibodies. The fluorescence intensities of CD69 in the CD4-positive and CD8-positive fractions are compared between the OK-432-stimulated DC transfer group and the immature DC transfer group. The data were obtained from six mice in each group. The histograms show the representative data. (b) The mean fluorescent intensities are also presented as the mean ± SE. *, P<0.05. (c) The antigen-specificities of the T-cell activations were confirmed by means of the IFN-γ ELISPOT assay using MC38 lysate. After CD4 or CD8 depletion using CD4 and CD8 magnetic beads, the lymphocytes from the draining lymph nodes were submitted to IFN-γ ELISPOT assay. Data were obtained from six mice in each group. *, P<0.05; **, P<0.01.
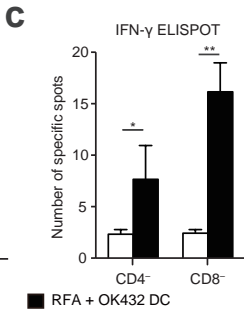
Figure 5: The augmented antitumor effects depended on both CD4-positive and CD8-positive cells. (a) For in vivo CD4 or CD8 depletion, monoclonal antibodies specific for CD4 (GK1.5) or CD8 (2.43), respectively, were injected intraperitoneally at 1 day before and 3 days after RFA. Tumor volumes were compared among the four groups for 10 days after RFA. In each experiment, data were obtained from four mice per group and are presented as the means ± SE. ns, not significant. (b) The draining lymph nodes were harvested at 3 days after RFA and analyzed for their

tumor-specificities using the IFN-γ ELISPOT assay. Two mice were used in each group. Data are shown as the mean ± SE. *, P<0.005; ns, not significant. (c) In the CD8 depletion study, splenocytes and tumor-infiltrating lymphocytes (TILs) were evaluated for their tumor-specificities using the IFN-γ ELISPOT assay as described in Fig. 3. Four mice were used in each group. Data are shown as the mean ± SE. ns, not significant.

a

	Phase	DiD	Merge

immature DC — No tx / Heat tx

OK432 DC — No tx / Heat tx

b

immature DC   OK432 DC

Relative cell number

DiD

---- Untreated MC38 —— Heat-treated MC38

c

% DiD+ cells / CD11c+ cells

immature DC   OK432 DC

ns

*   *

Untreated MC38
Heat-treated MC38

d

Draining lymph node

immature DC   OK432 DC

e

%GFP+CD11c+cell /lymphocyte

**

immature DC   OK432 DC

a

MC38 cells s.c. injection   RFA   DC injection
Day −7   Day 0   Day 1   Day 10

Observation period

Scar

b

Tumor volume (mm³)

1,200

900

600

300

0

0   3   7   10

Days after treatment

Day 10

Treatment

**

**

*

● ☐ No treatment
■ ☐ RFA only

▲ ▨ RFA + immature DC injection
▼ ■ RFA + OK432 DC injection

a

	No treatment	RFA only	RFA+immature DC	RFA+OK432 DC
CD4				
CD8				

b

CD4   CD8

Positive cell number/×400 field

*** *** ns

*** *** *** ns ***

Treatment

☐ No treatment ☐ RFA only
■ RFA + immature DC ■ RFA + OKDC

c

CD4   CD8   CD11c   NK1.1   Treg   MDSC

%Positive cells /Lymphocyte

ns *** *** ***   ns *** ** ***   ns   ns

Treatment

%CD4⁺CD25⁺Foxp3⁺/CD4⁺cells

ns ns *

Treatment

%CD11b⁺Gr-1⁺/Lymphocyte

ns

Treatment

☐ No treatment ☐ RFA only
■ RFA + immature DC ■ RFA + OK432 DC

d

IFN-γ ELISPOT

Number of specific spots

*** *** ***   *** *** **
ns   ns

Splenocyte   TIL

☐ No treatment ☐ RFA only
■ RFA + immature DC ■ RFA + OKDC

a

CD4

CD8

Relative cell number

CD69

$10^0 10^2$ 10^3 10^4 10^5 $10^0 10^2$ 10^3 10^4 10^5

---- RFA + immature DC —— RFA + OK432 DC

b

CD69 MFI

1000
800
600
400
200

* *

CD4   CD8

☐ RFA + immature DC   ■ RFA + OK432 DC

c

IFN-γ ELISPOT

Number of specific spots

20
15
10
5

* **

CD4⁻   CD8⁻

a

CD4 depletion

CD8 depletion

No treatment

RFA only

RFA + immature DC injection

RFA + OK432 DC injection

b

RFA + immature DC

RFA + OK432 DC

c

CD8 depletion study

No treatment

RFA + immature DC

RFA only

RFA + OK432 DC

Supplementary Figure 1

Effects of OK-432 on maturation of murine bone marrow-derived dendritic cells (DCs). Comparison of the mean fluorescence intensities (MFIs) of cell surface markers, murine major histocompatibility complex class II and CCR7 on OK-432-stimulated DCs and immature DCs. Data are shown as means ± SE. *, $P<0.05$. **, $P<0.001$.

Supplementary Figure 2

FITC-dextran uptake

Fluorescence intensity

Relative cell number

MFI

**

☐ immature DC   ■ OK432 DC
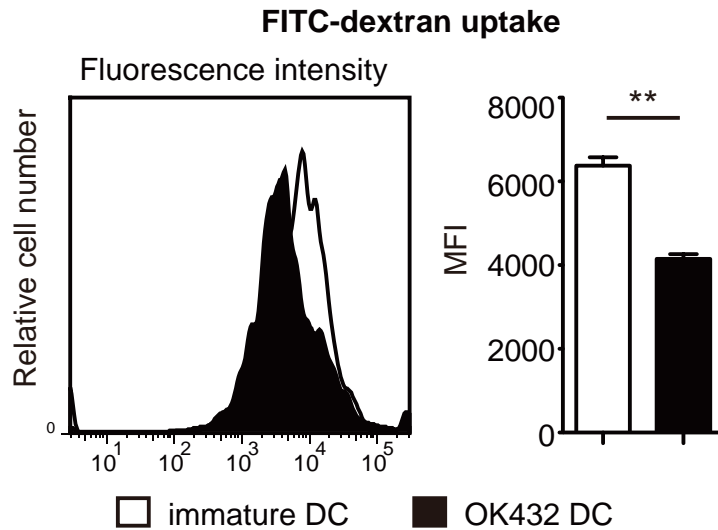
Dendritic cells (DCs) with or without OK-432 stimulation were incubated with fluorescein isothiocyanate (FITC)-dextran for 30 minutes and the uptakes were examined using flow cytometry. DCs were also stained with anti-CD11c antibody. Representative results are shown as histograms and median fluorescence intensities. The open area represents immature DCs and the filled area represents OK-432-stimulated DCs. The experiments were performed six times and the results were confirmed. The data are presented as the mean ± SE. **, P<0.001.

Supplementary Figure 3
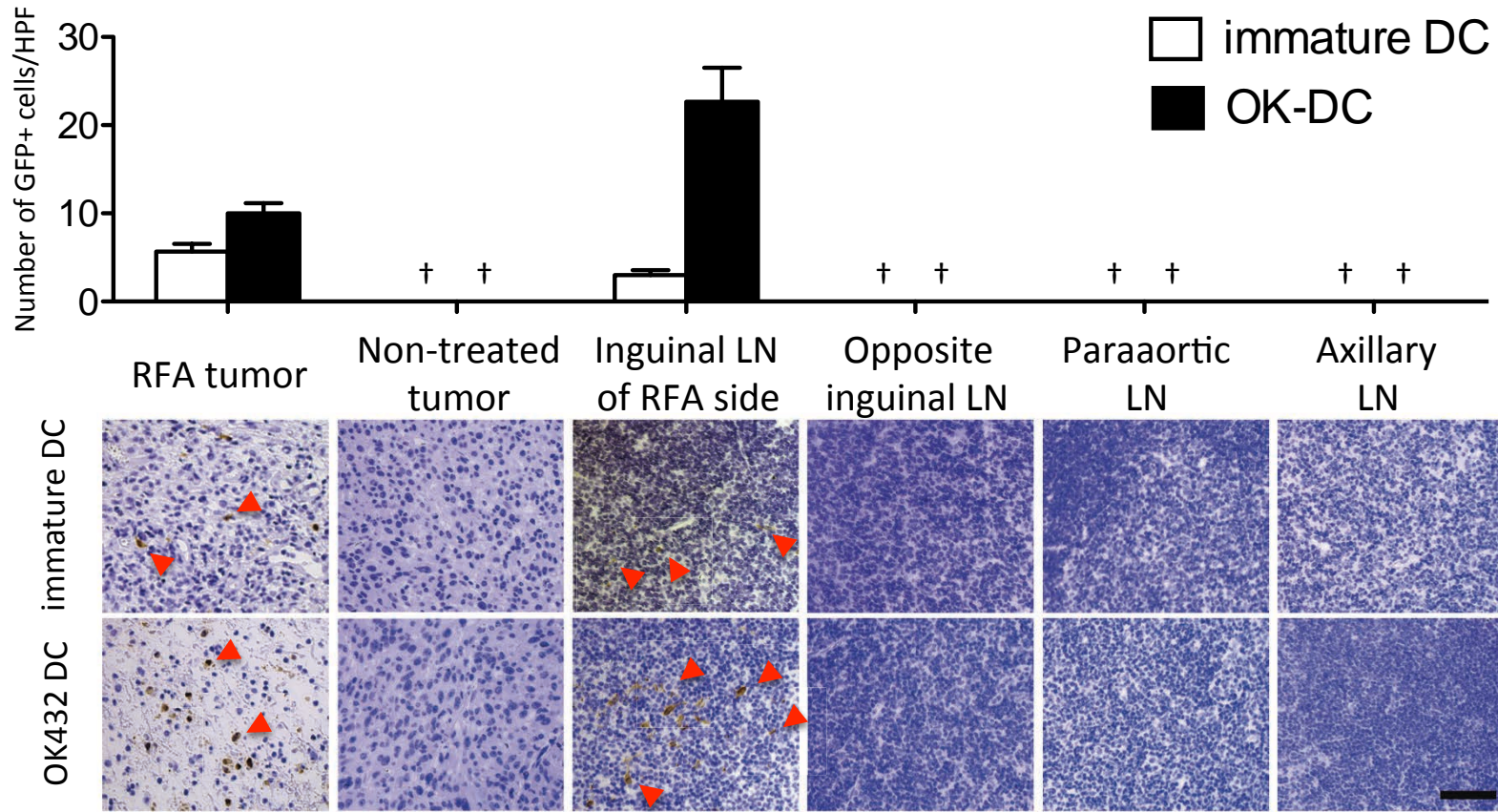
Kinetics of transferred dendritic cells (DCs) were evaluated using immunohistochemistry. Each organ was stained with anti-GFP antibodies and GFP-positive cells were counted at 3 days after RFA treatment, followed by the injection of immature or OK-432-stimulated DCs. Data are shown as the mean ± SE. Bar, 50 μm; †not detected; arrowheads, GFP positive cells; LN, lymph node.
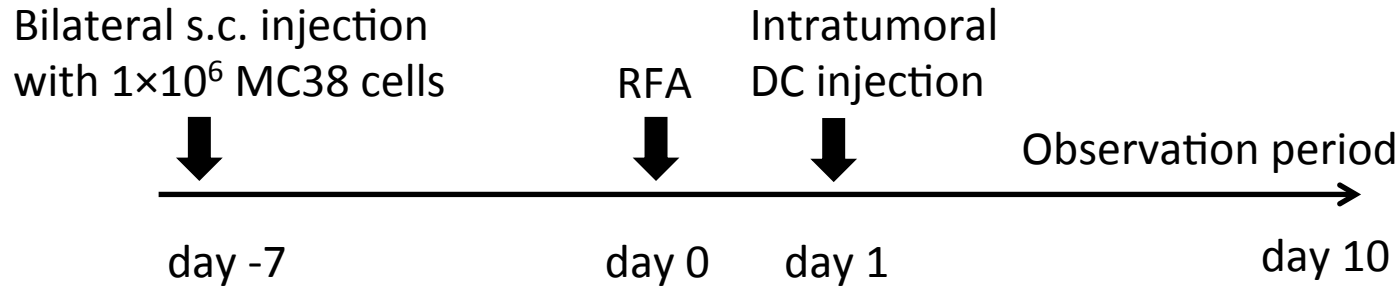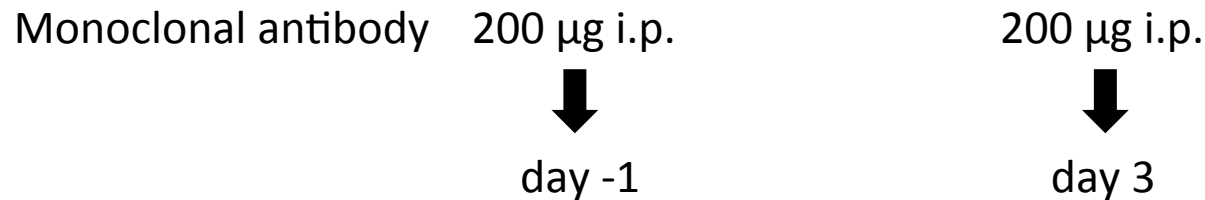
Supplementary Figure 4
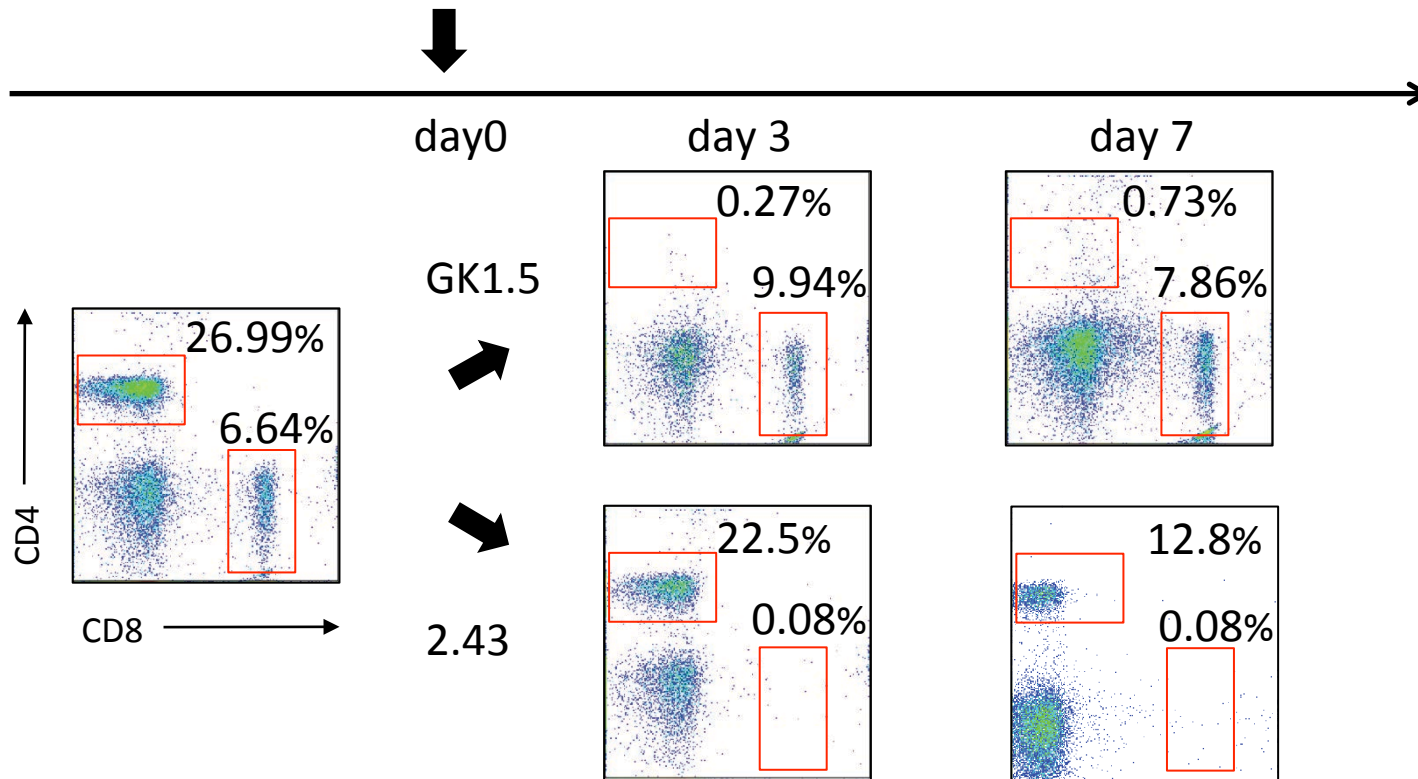
In vivo CD4/CD8 depletion was performed by means of i.p. injection of GK1.5 or 2.43 monoclonal antibodies. To confirm the depletion of T-cell subsets, peripheral blood lymphocytes were stained with anti-CD4 antibodies (Ab) and ant-CD8 Ab, and analyzed using flow cytometry at 3 days and 7 days after i.p. injection of 200 μg monoclonal Abs.

Supplementary Figure 5

Bilateral s.c. injection
with 1×10^6 MC38 cells

RFA

Intratumoral
DC injection

Observation period

day -7   day 0   day 1   day 10

For CD4/CD8 depletion

Monoclonal antibody   200 µg i.p.   200 µg i.p.

day -1   day 3

In vivo treatment model is described above. RFA was applied to a tumor on one side, when subcutaneous tumors grew up to about 5 mm in diameter, followed by injection of 1×10^7 DCs into the treated tumor with RFA. Untreated tumor on the opposite side was observed for 10 days. For in vivo CD4/CD8 depletion, 200 µg of the monoclonal antibodies, clone GK1.5 or clone 2.43 were i.p. injected 1 d before and 3d after RFA treatment.

Supplementary Figure 6
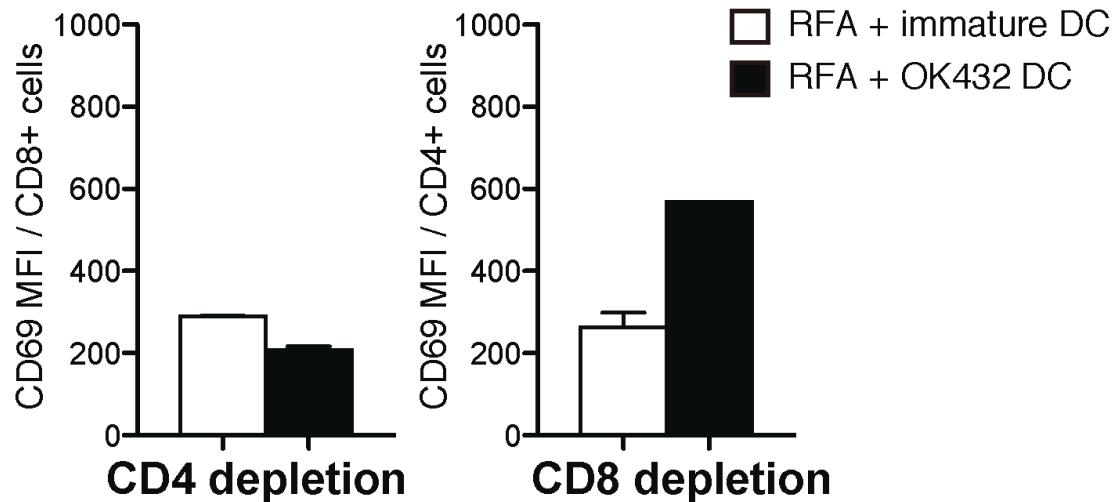
In the CD4/CD8 depletion studies, the draining lymph nodes were harvested at 3 days after radiofrequency ablation (RFA), and their activations and antigen-specificities were evaluated. The mean fluorescent intensities of CD69 in CD8-positive cells from the CD4-depleted mice and CD4-positive cells from the CD8-depleted mice were estimated. Two mice were used in each group. Data are presented as the mean ± SE.